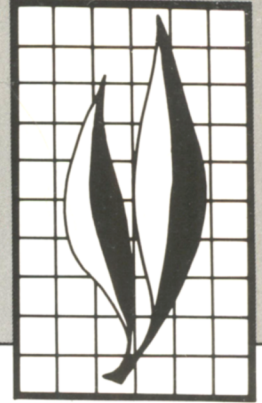


Hilgardia

A JOURNAL OF AGRICULTURAL SCIENCE PUBLISHED BY
THE CALIFORNIA AGRICULTURAL EXPERIMENT STATION



Volume 55 • *Number 4* • *July 1987*

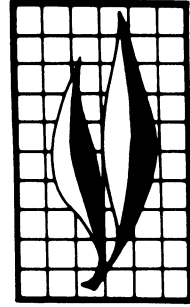
The Spatial Variability of Water and Solute Transport Properties in Unsaturated Soil

I. Analysis of Property Variation and Spatial Structure with Statistical Models

William A. Jury, David Russo, Garrison Sposito, and Hesham Elabd

II. Scaling Models of Water Transport

William A. Jury, David Russo, and Garrison Sposito



ABSTRACTS

I. Analysis of Property Variation and Spatial Structure with Statistical Models

This review presents and examines relevant information from existing spatial variability studies of soil water and solute transport properties. Although most of the information available allowed only a conventional statistical analysis (mean and variance) of the pertinent properties, the field studies of Nielsen, Biggar, and Erh (1973) and Russo and Bresler (1981) were also suitable for spatial structure analysis. Detailed structural analysis of the saturated hydraulic conductivity (K_s) of these two fields demonstrated how this type of analysis may reveal field characteristics that are not apparent from conventional statistical analysis.

Using the Akaike Information Criterion for model discrimination, the three-dimensional spatial distributions of $\ln K_s$ of both fields were shown to be described best by a spherical covariance function and a linear drift function. The Hamra field of Russo and Bresler (1981) had a much larger deterministic drift component and a smaller stochastic

Continued inside back cover.

THE AUTHORS:

William A. Jury is Professor of Soil Science and Soil Physicist, Department of Soil and Environmental Sciences, University of California, Riverside.

David Russo was Visiting Scientist in the Department of Soil and Environmental Sciences, University of California, Riverside, from 1984 to 1986. He has since returned to his position as Soil Physicist at the Volcani Center, Agricultural Research Organization, Bet-Dagan, Israel.

Garrison Sposito is Professor of Soil Science and Soil Chemist, Department of Soil and Environmental Sciences, University of California, Riverside.

Hesham Elabd, former Graduate Research Assistant in the Department of Soil and Environmental Sciences, University of California, Riverside, is now Postdoctoral Researcher at New Mexico State University, Las Cruces.

II. Scaling Models of Water Transport

INTRODUCTION

TILLOTSON AND NIELSEN (1984) and Sposito and Jury (1985) have shown that the behavior of water in the vadose zone may be analyzed by more than one scaling technique. The philosophy behind the application of scaling methods to water in field soils has been either to simplify the task of making replicate measurements on a field or to help calibrate a field-wide transport model formulated from scaling relationships (Warrick and Nielsen 1980). Current scaling approaches to the unsaturated zone have evolved principally from the theory of microscopic geometric similitude first proposed by Miller and Miller (1956). In this theory, two porous media, or two regions of a single porous medium (as in a field soil) are termed "similar" if their microscopic geometric structures are identical except for a difference in magnification, and if the same physical mechanisms underlie the behavior of water in them. To represent the relative magnification in quantitative terms, each region is assigned a scaling length λ that represents a characteristic microscopic dimension. Since both porous media, or both regions in a porous medium, are assumed to obey microscopic transport laws based on viscous flow and capillary forces (Miller and Miller 1956), the macroscopic transport coefficients for the two media or regions are related by known functions of their scaling lengths. These functions can be deduced from the microscopic transport laws. To remove the explicit dependence of scaled transport coefficients on the microscopic length parameter, the transport coefficients in a given medium or at a given point in a medium are related to the coefficients at an arbitrary reference point (denoted by an asterisk) through scaling length ratios $\alpha = \lambda/\lambda^*$ (*scaling factors*). Functional relationships for soil water properties that follow directly from this scaling theory are given in table 1 (Miller 1980).

Tests of microscopic geometric similitude have been performed in the laboratory on packed columns of spherical glass beads, well-sorted sands, and soils (Miller 1980; Tillotson and Nielsen 1984). In the experiments with glass beads and sands, the microscopic characteristic length λ was determined directly by preparing each column with particles from a different predetermined size fraction. Separate tests of functional relationships (Klute and Wilkinson 1958) and dynamic transport behavior (Elrick, Sandrett, and Miller 1959; Wilkinson and Klute 1959) were described successfully by microscopic scaling theory. In tests of microscopic scaling theory using columns of soil, however, the parameter λ could no longer be measured directly, but had to be inferred from texture measurements. These tests indicated that microscopic scaling theory does not apply well to soils containing a broad range of particle sizes or exhibiting a significant variability in water content (Tillotson and Nielsen 1984).

In respect to field soils, the difficulties faced in the microscopic geometric similitude technique are compounded by the requirement of this approach that the water content at saturation have a uniform value throughout the field (Miller 1980), a condition that

is seldom, if ever, met in practice (Jury 1985). Because of these fundamental problems, a scaling approach termed *functional normalization* by Tillotson and Nielsen (1984) or *macroscopic Miller similitude* by Sposito and Jury (1985) has been developed. In this approach, no hypotheses concerning the microscopic geometric structure of a porous medium are made, but the formal scaling relationships in table 1 are retained for soil water potentials and transport coefficients. The volumetric water content is not assumed to be a uniform property and is scaled by the porosity, so that the relative saturation $s = \theta/\phi$ (or an equivalent variable) is used as a water content parameter in scaling relationships. Scaling factors determined by measurements of different soil water properties at the same location may be compared as a test of the validity of macroscopic Miller similitude for real soils (Bresler, Russo, and Miller 1978; Reichardt, Libardi, and Nielsen 1975; Reichardt, Nielsen, and Biggar 1972; Youngs and Price 1981). This kind of test has indicated that macroscopic scaling theory can apply well to column studies of soils comprising a broad distribution of particle sizes and water contents (Sposito and Jury 1985; Tillotson and Nielsen 1984).

Table 2 presents the results of field studies (Rao et al. 1983; Russo and Bresler 1980; Sharma, Gander, and Hunt 1980; Simmons, Nielsen, and Biggar 1979; Warrick, Mullen, and Nielsen 1977) in which scaling factors were determined indirectly by two different methods, then normalized and compared by examining their degree of statistical correlation. The high degree of correlation observed in most studies may seem to support the hypothesis of macroscopic Miller similitude for the fields investigated. With the exception of the studies by Russo and Bresler (1980) and Simmons, Nielsen, and Biggar (1979), however, the statistical relationship between the two scaling factors was not linear, and the sample variances of the two scaling factor distributions were not the same.

In table 3, the sample log mean (μ) and log standard deviation (σ) for scaling factors measured in field studies are compared. Each distribution was fitted to a lognormal distribution and normalized to have unit mean value. Along with the statistics μ and σ , table 3 gives the sample coefficient of variation (CV) and the range of values ($\alpha_{.05}$,

TABLE 1. FUNCTIONAL RELATIONSHIPS FOR SOIL PROPERTIES
BASED ON MICROSCOPIC GEOMETRIC SIMILITUDE

Soil property	Scaling relationship [†]
Porosity	$\phi^* = \phi$
Volumetric water content	$\theta^* = \theta$
Bulk density	$\rho_b^* = \rho_b$
Matric potential	$b^*(\theta^*) = \alpha b(\theta)$
Hydraulic conductivity	$K^*(\theta^*) = \alpha^{-2}K(\theta)$
Water diffusivity	$D^*(\theta^*) = \alpha^{-1}D(\theta)$
Sorptivity	$S^*(\theta^*) = \alpha^{-1/2}S(\theta)$
Philip A parameter [‡]	$A^*(\theta^*) = \alpha^{-2}A(\theta)$
Steady-state infiltration rate	$i_{\infty}^* = \alpha^{-2}i_{\infty}$

[†]Based on microscopic geometric similitude and the scaling length ratio $\alpha = \lambda/\lambda^*$, where * denotes a reference location.

[‡]See equation 2 and Philip (1969).

$\alpha_{.95}$) which encompass 90 percent of the probability distribution, the latter being calculated from the formula

$$\alpha_{.95} = \exp(\mu \pm 1.64\sigma) \tag{1}$$

(Hald 1952). Comparing the same studies in tables 2 and 3, we find large differences between scaling factor distributions estimated by different procedures that are not reflected in the high correlation coefficients given in table 2. For example, the hydraulic conductivity and matric potential scaling factors determined in the study of Warrick, Mullen, and Nielsen (1977) are highly correlated ($r^2 = 0.83$), but have very different log variances ($\sigma^2 = 1.17$ and $\sigma^2 = 0.51$, respectively) and different limits bounding 90 percent of their probability distribution ([0.07, 3.42] and [0.38, 2.02], respectively). Similarly, the highly correlated ($r^2 = 0.83$) S and A scaling factors in the study of Sharma, Gander, and Hunt (1980), which were obtained from scaling the infiltration rate i based on the Philip equation

$$i = \frac{1}{2} S t^{-1/2} + A \tag{2}$$

(Philip 1969), have log variances $\sigma^2 = 1.06$ and $\sigma^2 = 0.33$, respectively. For these two parameters, the range of α -values encompassing 90 percent of the distribution are, respectively, (0.10, 3.25) and (0.55, 1.62).

The comprehensive field experiment of Nielsen, Biggar, and Erh (1973) provides an opportunity to illustrate the limited applicability of macroscopic Miller similitude to their study. At each of the 20 sites and 6 depths in their investigation, four different properties were measured from which scaling factors could be calculated. These methods are listed as the first four entries in table 3. Each of the scaling factor distributions derived from the four methods may be used to calculate the distribution of soil properties using the relationships given in table 1. The procedure may be illustrated by focusing on two properties of interest: the unsaturated hydraulic conductivity

TABLE 2. CORRELATION BETWEEN SCALING FACTORS OBTAINED BY TWO EXPERIMENTAL METHODS FOR THE SAME FIELD

Method A	Method B	N*	r^2_{AB} †	Reference
Scale matric potential	Scale hydraulic conductivity	120	0.83	Warrick, Mullen, and Nielsen 1977
Scale matric potential	Scale hydraulic conductivity	8	0.80	Simmons, Nielsen, and Biggar 1979
Scale matric potential	Scale hydraulic conductivity	120	0.86	Russo and Bresler 1980
Scale matric potential	Scale hydraulic conductivity	50	≈ 0	Rao et al. 1983
Scale S in Philip equation	Scale Philip A parameter	26	0.83	Sharma, Gander, and Hunt 1980
Scale wetting front by $K(b)$ model function	Scale wetting front by Philip equation	120	0.57	Russo and Bresler 1980

*N = number of measurements.

† r^2_{AB} = serial correlation coefficient.

TABLE 3. SCALING FACTOR λ DISTRIBUTION PARAMETERS FOR $y = \ln \lambda$ (MEAN μ , VARIANCE σ^2) AND COEFFICIENT OF VARIATION CV FOR λ OBTAINED FROM FIELD STUDIES (THE VALUES $\alpha_{.05}$ AND $\alpha_{.95}$ REPRESENT THE LOWEST AND HIGHEST FIVE PERCENT OF THE POPULATION)

Soil texture	Field size	Number	μ_y	σ_y	CV	$\alpha_{.05}$, $\alpha_{.95}$	Method*	Reference
Clay loam	150 ha	120 (6 depths)	-0.13	0.51	55	0.38, 2.03	A	Warrick, Mullens, and Nielsen 1977
		120	-0.62	1.17	170	0.07, 3.42	B	Warrick, Mullens, and Nielsen 1977
		120	-0.49	0.99	130	0.12, 3.11	C	Warrick, Mullens, and Nielsen 1977
		120	-0.14	0.59	64	0.33, 2.29	D	Nielsen, Biggar, and Erh 1973
Loam	87 ha	180 (5 depths)	-0.10	0.45	48	0.43, 1.89	A	Warrick, Mullens, and Nielsen 1977
Loam	within 7 km	64 (8 depths)	-0.54	1.04	139	0.11, 3.21	A	Warrick, Mullens, and Nielsen 1977
Silt loam	9.6 ha	26	-0.56	1.06	143	0.10, 3.25	E	Sharma, Gander, and Hunt 1980
		26			34	0.55, 1.63	F	Sharma, Gander, and Hunt 1980
Sand	0.8 ha	120	-0.05	0.30	31	0.58, 1.56	A	Russo and Bresler 1980
		120	-0.13	0.51	55	0.38, 2.03	B	Russo and Bresler 1980
		120	-0.16	0.57	62	0.33, 2.17	G	Russo and Bresler 1980
		120	-0.08	0.41	43	0.47, 1.81	H	Russo and Bresler 1980
Loam	0.7 ha	72 (6 depths)	-0.38	0.77	90	0.19, 2.42	A	Simmons, Nielsen, and Biggar 1979

*A scale $b(\theta)$;

B scale $K(\theta)$;

C calculated from K_o in $K = K_o \exp(b\theta)$ measured during redistribution;

D scale steady-state infiltration;

E scale S in Philip infiltration equation;

F scale A in Philip infiltration equation;

G scale wetting front distance using model $K(b)$ function;

H scale wetting front distance using Philip infiltration equation.

$K(s)$ and the matrix potential $b(s)$ at 90 percent saturation. From table 1, we learn that $K(s)$ is related to the reference-state hydraulic conductivity $K^*(s)$ by the equation

$$K(s) = \alpha^2 K^*(s). \tag{3}$$

Since α is assumed to follow a lognormal distribution, $K(s)$ is also lognormally distributed. Letting $y = \ln\alpha$ and $z = \ln K(s)$ be normal variates with mean and variance (μ_y, σ_y^2) and (μ_z, σ_z^2) , respectively, the following relationships may be deduced from equation 3:

$$E[\ln K(s)] = \mu_z = \ln[K^*(s)] + 2\mu_y, \tag{4a}$$

and

$$\text{Var}[\ln K(s)] = \sigma_z^2 = 4\sigma_y^2. \tag{4b}$$

The reference conductivity $K^*(s)$ is defined by the requirement that α have unit mean value and that $\lambda = 1$ at the reference location, which results in the condition

$$K^*(s) = \left\{ \int_0^\infty [K(s)]^{1/2} f[K(s)] dK \right\}^2 \tag{5a}$$

(Peck, Luxmoore, and Stolzy 1977; Russo and Bresler 1980). The integral in equation 5a may be evaluated directly using equation 4

$$K^*(s) = \exp(\mu_z + \sigma_z^2/4) = E[K(s)] \exp(-\sigma_z^2/4) \tag{5b}$$

(Hald 1952), or, using equation 4b,

$$K^*(s) = E[K(s)] \exp(-\sigma_y^2), \tag{5c}$$

where $\mu_y = -\sigma_y^2/2$ from the requirement that $E[\alpha] = 1$.

The relationships in equation 4, together with known properties of the lognormal distribution (Aitchison and Brown 1976), can be used to derive the major statistical properties of the $K(s)$ distribution in terms of the parameters of the y distribution and K^* :

$$\text{Median}[K(s)] = \exp(\mu_z) = K^*(s) \exp(-\sigma_y^2) \tag{6}$$

$$\text{Mode}[K(s)] = \exp(\mu_z - \sigma_z^2) = K^*(s) \exp(-5\sigma_y^2) \tag{7}$$

$$\text{Mean}[K(s)] = \exp(\mu_z + \sigma_z^2/2) = K^*(s) \exp(\sigma_y^2) \tag{8}$$

$$\begin{aligned} \text{Var}[K(s)] &= \exp(2\mu_z + \sigma_z^2) [\exp(\sigma_z^2) - 1] \\ &= [K^*(s)]^2 \exp(2\sigma_y^2) [\exp(4\sigma_y^2) - 1] \end{aligned} \tag{9}$$

$$\begin{aligned} \text{CV}[K(s)] &= [\exp(\sigma_z^2) - 1]^{1/2} \\ &= [\exp(4\sigma_y^2) - 1]^{1/2}. \end{aligned} \tag{10}$$

Similar results may be derived for $b(s)$ using the scaling relationship

$$b(s) = \alpha^{-1} b^*(s) \tag{11a}$$

where b^* is defined by the equation

$$b^*(s) = \left\{ \int_{-\infty}^0 [b(s)]^{-1} f[b(s)] db \right\}^{-1} \tag{11b}$$

(Peck, Luxmoore, and Stolzy 1977; Russo and Bresler 1980), or, using equation 11a,

$$b^*(s) = E[b(s)] \exp(-\sigma_y^2). \tag{11c}$$

The data in table 4 summarize the statistical properties of $K(s)$ and $b(s)$ at $s = 0.9$, calculated for each of the four scaling-factor distributions determined with data obtained in the study of Nielsen, Biggar, and Erh (1973). For each of the four methods, $K^*(0.9)$ and $b^*(0.9)$ were calculated from equations 5b and 11c, using $E[K(0.9)] = 0.122$ cm per hour and $E[b(0.9)] = -64.4$ cm, respectively. The large differences in the statistical properties offer convincing evidence that macroscopic Miller similitude was not applicable in this study. Furthermore, the scaling factor distribution obtained by scaling $K(s)$ in the study of Warrick, Mullen, and Nielsen (1977) (method B in table 4) produces $K(s)$ and $b(s)$ distributions that have coefficients of variation (CV) five to ten times larger than any sample CVs observed previously for these properties in any field reviewed in Part I of this study (Jury et al. 1987) or by Jury (1985).

It is apparent that the assumptions underlying macroscopic Miller similitude may not be valid for describing typical field soil heterogeneity. Although it has been pointed out (Sposito and Jury 1985; Tillotson and Nielsen 1984) that macroscopic Miller similitude represents but one hypothesis that can be made in scaling soil water phenomena, several theoretical models that have been proposed for describing field-scale water and chemical transport are based explicitly on the assumption that macroscopic Miller similitude is a valid means of coalescing spatially variable characteristics into a unified representation. Warrick and Amoozegar-Fard (1980) scaled the Richards

TABLE 4. STATISTICAL PROPERTIES OF K AND b AT 90 PERCENT SATURATION CALCULATED FROM SCALING FACTOR DISTRIBUTIONS ($y = \ln \lambda$) FOR THE FIELD OF NIELSEN ET AL. (1973)†

Method‡	μ_y	σ_y	K^*	Mode[K]	Med[K]	Var[K]	CV [§]
				-----cm h ⁻¹ -----		cm ² h ⁻²	%
A	-0.13	0.51	0.094	0.026	0.072	0.027	135
B	-0.62	1.17	0.027	3.27×10^{-5}	0.008	3.539	1,542
C	-0.49	0.99	0.046	3.42×10^{-4}	0.017	0.731	701
D	-0.14	0.59	0.080	0.015	0.061	0.045	174
Method‡	μ_y	σ_y	b^*	Mode[b]	Med[b]	Var[b]	CV [§]
				-----cm H ₂ O-----		cm ²	%
A	-0.13	0.51	64.4	56.5	73.3	1,231	54.5
B	-0.62	1.17	60.4	28.6	112.2	12,155	171.2
C	-0.49	0.99	64.4	39.4	105.1	6,902	129.0
D	-0.14	0.59	62.2	50.5	71.5	1,727	64.5

Actual K^ and b^* are defined in equations 3 and 11a, b, and c.

†Actual sample variances of $K(0.9)$ and $b(0.9)$ are $0.0589 \text{ cm}^2 \text{ h}^{-2}$ and $1,106 \text{ (cm H}_2\text{O)}^2$, respectively.

‡See table 3.

§CV = coefficient of variation.

equation for water flow and showed that a single numerical calculation for representative soil water processes, such as infiltration or drainage, could be used along with a distribution of scaling factors to produce a fieldwide description of the processes, using the assumption of one-dimensional flow. Bresler and Dagan (1979, 1981, 1983a, b; Dagan and Bresler 1979, 1983) have proposed stochastic water and solute transport models in which a theoretical scaling probability distribution was used together with a local one-dimensional vertical water and solute transport model to produce stochastic expectation and variance values for solute concentrations averaged across the entire cross-sectional area of a field at a given depth. Neither of these theories has had quantitative experimental confirmation. The only direct test of the predictive capability of soil water transport models that use macroscopic Miller similitude was conducted by Luxmoore and Sharma (1980), who obtained scaling factors for six watersheds, and then simulated drainage, evaporation, and runoff processes using the regional-scale hydrologic water balance model of Huff et al. (1976). They reported poor agreement between observed streamflow and predicted runoff for the fields they studied.

Russo and Bresler (1982) compared solutions of stochastic-conceptual flow problems by utilizing the scaling factor α as a single stochastic parameter, with solutions obtained by using a multivariate parameter distribution to describe the spatial variability of hydraulic properties. They analyzed two cases of one-dimensional vertical flow: (1) piston flow of solute under a steady and, over the horizontal plane, uniform surface water application rate; and (2) transient water flow under a uniform surface water application rate. Using the measured hydraulic properties of the Hamra field (Russo and Bresler 1981), they concluded that, for case 1, expressing the variability in $K(\theta)$ by the single stochastic variable α gives essentially the same results as when the variability in $K(\theta)$ is expressed by three stochastic variables. In case 2, they found that in expressing the variability in $K(\theta)$ and $b(\theta)$ only by α they failed to reconstruct the distribution of the θ -profiles obtained by expressing the spatial variability in $b(\theta)$ and $K(\theta)$ by five stochastic variables.

A common feature of all scaling models used up until now for field applications is the assumption of statistical independence for the measured scaling factors. Yet, both water transport and retention properties have been observed to correlate spatially over distances of many meters (Jury et al. 1987), so that the assumption of statistical independence may be contributing to the lack of success of these models.

In the remainder of this paper, we will develop a more general scaling analysis that includes spatial correlation structure, illustrated with data from two comprehensive field studies (Nielsen, Biggar, and Erh 1973; Russo and Bresler 1981).

SCALING AND SPATIAL CORRELATION

We will apply the methodologies presented in Part I (Jury et al. 1987) for selection of a model to describe the spatial variability of the scaling factors derived from measurements of the soil hydraulic conductivity or water retentivity functions. The results of the selection process for the Hamra (Russo and Bresler 1981) and Panoche (Nielsen, Biggar, and Erh 1973) fields will be demonstrated. As in Part I, we view the scaling factor as a realization of a three-dimensional, isotropic stochastic function. Two different models (equations 25a and 25b of Part I) will be considered for the covariance

function, and constant and linear drift functions (equation 26 with $K = 1$ and $K = 3$, respectively, from Part I) will be used for both $u = \alpha$ and $u = \ln\alpha$. The Akaike Information Criterion (AIC) will be used to discriminate among the different proposed spatial variability models.

Hamra Field

With the 120 measured values (Russo and Bresler 1981) of the saturated hydraulic conductivity K_s , air entry value b_w , saturated water content θ_s , and residual water content θ_r , calculations were made of the water retentivity function $b(\theta)$ and the soil hydraulic conductivity function $K(\theta)$ from the model functions

$$b(\theta) = b_w \theta^{-1/\beta} \tag{12a}$$

and

$$K(\theta) = K_s \theta^{(2 + m + 2/\beta)} = K_s \theta^\epsilon, \tag{12b}$$

where θ is the effective water saturation given by

$$\theta = (\theta - \theta_r)/(\theta_s - \theta_r), \tag{12c}$$

β is a model parameter, and m is a constant (positive or negative) that accounts for correlation between pore size and flow path tortuosity. Based on laboratory tests of equation 12, Russo and Bresler (1981) used $m = 0$, which is identical to the series-parallel model of Childs and Collis-George (1950).

Values of $K(\theta)$ and $b(\theta)$ calculated from equations 12a and 12b at 11 values of the water saturation $s = \theta/\theta_s$ ($s_i = 1.0 - 0.025 [i - 1]$, for $i = 1$ to $i = 11$) were used to calculate two sets of scaling factors α_K and α_b , respectively. The data in table 5 summarize some statistical properties of the calculated $K(s)$ and $b(s)$ values and their logarithmic transformations. The scaling factor sets were calculated using a procedure similar to that of Warrick, Mullen, and Nielsen (1977), but with K^* and b^* defined by equations 5a and 11b, respectively, and estimated from a sample size of n using either the equation

$$\hat{K}^*(s) = \left[\sum_{j=1}^n [K_j(s)]^{1/2} / n \right]^2 \tag{13a}$$

or the equation

$$\hat{b}^*(s) = n \left[\sum_{j=1}^n 1/b_j(s) \right]^{-1} \tag{13b}$$

instead of the arbitrary functional relationships used by Warrick, Mullen, and Nielsen. Also, since both $b(s)$ and $K(s)$ are highly variable (table 5), transformed values of $\ln b(s)$ and $\ln K(s)$ (as in Russo and Bresler 1980) were used instead of $b(s)$ and $K(s)$, as in Warrick, Mullen, and Nielsen (1977), to estimate α_b and α_K , respectively.

In table 6, we summarize the results of a conventional statistical analysis of α_b , $\ln\alpha_b$, α_K and $\ln\alpha_K$ based on a sample size of $n = 120$. Both the chi-square test and

the Kolmogorov-Smirnov (KS) test results accept the null (normal distribution) hypothesis for α_b and α_K , but reject the null hypothesis for both $\ln\alpha_b$ and $\ln\alpha_K$. Generally, the two sets of α vary between 0.0 and 2.7 and are relatively highly correlated ($R^2 = 0.66$, with intercept -0.1802 and slope 1.180). Note, however, that this regression analysis assumed both α_b and α_K to be independent variates. In the following analysis, we will see the methodology described in Part I (Jury et al. 1987) to investigate the spatial correlation structure of both α_b and α_K . We will then use the selected structural models to transfer the vector α of each of the sets to a vector of uncorrelated residuals.

TABLE 5. STATISTICAL CHARACTERISTICS (MEAN, COEFFICIENT OF VARIATION CV, AND VARIANCE σ^2 OF THE LOG-TRANSFORMED PARAMETER) OF THE HYDRAULIC PROPERTIES OF HAMRA FIELD FOR DIFFERENT DEGREES OF WATER SATURATION s^*

Water saturation s	K			b		
	Mean	CV [†]	$\hat{\sigma}^2_{\ln K}$	Mean	CV [†]	$\hat{\sigma}^2_{\ln b}$
	<i>cm/hr</i>			<i>cm H₂O</i>		
1.0	13.19	0.69	1.033	7.44 [‡]	0.24	0.0653 [‡]
0.975	11.11	0.77	1.457	8.28 [‡]	0.24	0.0577 [‡]
0.950	9.45	0.84	2.018	9.40	0.31	0.0786 [‡]
0.925	8.08	0.92	2.734	10.96	0.47	0.1315 [‡]
0.900	6.94	0.98	3.623	13.23	0.72	0.2204
0.875	5.97	1.04	4.709	16.71	1.06	0.3502
0.850	5.14	1.10	6.019	22.35	1.49	0.5265
0.825	4.43	1.16	7.583	32.10	2.01	0.7561
0.800	3.81	1.22	9.442	49.84	2.57	1.047
0.775	3.27	1.27	11.640	84.36	2.66	1.409
0.750	2.80	1.33	14.230	155.80	3.70	1.854

*Based on sample of $n = 120$.

[†]CV = coefficient of variation.

[‡]Null (normal) hypothesis is not rejected at the 0.05 level of significance (χ^2 test).

TABLE 6. CONVENTIONAL STATISTICAL ANALYSIS OF THE SCALING FACTOR SETS (HAMRA FIELD) CONSIDERING ALL FOUR DEPTHS JOINTLY ($n = 120$)^{*}

Parameter	$\hat{\mu}$	$\hat{\sigma}^2$	\hat{k}_s	\hat{k}_c	$\chi^2(df)$	D
α_b	1.000	0.2157	0.293	4.183	2.80 (3)	0.0641
$\ln\alpha_b$	-0.1667	0.4684	-1.740	6.231	39.40 (3) [†]	0.1580 [‡]
α_K	1.000	0.4558	0.334	2.183	7.20 (3)	0.08122
$\ln\alpha_K$	-0.426	1.401	-1.496	4.965	49.30 (3) [†]	0.1354 [‡]

*Mean μ , σ^2 , skew coefficient k_{sk} , coefficient of kurtosis k_c , chi-square χ^2 , and KS statistic D.

[†]Null (normal) hypothesis is rejected at the 0.05 level of significance.

[‡]Null (normal) hypothesis is rejected at the 0.10 level of significance.

Based on the results of the conventional statistical analysis (table 6), the spatial structures of α_b and α_K were analyzed instead of their logarithmic transformations. As in Part I, four candidate structural models were applied to the α -sets: exponential covariance plus constant drift ($E + C$) and linear drift ($E + L$) and spherical covariance plus constant drift ($S + C$) and linear drift ($S + L$). The restricted maximum likelihood (RML) estimation procedure (Kitanidis and Lane 1985) was used to estimate the parameters of the assumed covariance function, and the weighted least squares analysis (WLS, equation 27 in Part I) was used to estimate the parameters of the assumed drift function. We performed cross-validation tests and an analysis of the uncorrelated residuals to evaluate the performance of each of these models; the most appropriate model was selected as the one that minimized the value of the AIC (equation 28 in Part I). For α_b , the $E + C$, $S + C$, $E + L$, and $S + L$ models produced AIC values of 77.6, 76.5, 38.3, and 38.5, respectively. For α_K , the same models produced AIC values of 123.2, 120.8, 61.5, and 60.7, respectively. Thus, the $E + L$ and the $S + L$ models were selected for α_b and α_K , respectively.

In table 7 the results of structural analysis, the cross-validation test, and the analysis of uncorrelated residuals for these two models are compared. Evidently, the spatial structures of α_b and α_K are quite distinct. The cross-validation test and the analysis of the uncorrelated residuals suggest that, in both cases, the models selected are consistent with the data. The latter test also accepts the assumption of normality for both α_b and α_K . In both cases, the linear drift model was found to be highly significant ($R^2 =$

TABLE 7. ANALYSIS OF THE SPATIAL VARIABILITY OF α_b AND α_K USING $n = 60$ VALUES OF BOTH α -SETS RANDOMLY SELECTED FROM THE FOUR DIFFERENT SOIL DEPTHS (HAMRA FIELD)*

<i>a. Structural analysis</i> [†]								
Parameter	Model	\hat{C}_n	\hat{C}_o	\hat{a}				
α_b	$E + L$	0.0592 (.025)	0.0399 (.019)	2.095 (2.42)				
α_K	$S + L$	0 (—)	0.1446 (.028)	0.761 (.199)				

<i>b. Cross validation</i> [‡]				
Parameter	Model	ME	MSE	MRE
α_b	$E + L$	0.0251	0.3579	1.246
α_K	$S + L$	-0.0110	0.3777	1.142

<i>c. Analysis of uncorrelated residuals</i> [§]								
Parameter	Model	$\hat{\mu}$	$\hat{\sigma}^2$	\hat{k}_{sk}	\hat{k}_c	$\chi^2(df)$	D	SSR
α_b	$E + L$	0.1496	0.9396	0.315	2.23	2.3 (3)	0.07512	57.08
α_K	$S + L$	0.1441	0.9791	-0.210	2.63	5.1 (3)	0.1032	5.00

*Values in parentheses are the standard error of estimation (SE). If the value is zero, there is no standard error.

[†] \hat{C}_n is nugget variance, \hat{C}_o is covariance, \hat{a} is covariance shape parameter.

[‡]ME is mean error, MSE is mean square error, MRE is mean reduced error.

[§]SSR is sum of squares of residuals. Other symbols are defined in table 6.

0.901 and $R^2 = 0.895$ for α_b and α_K , respectively). In the case of α_b , the deterministic low-frequency variations (LFV, the drift contribution) of α_b are characterized by the variance contribution $\hat{C}_D = 0.1093$ (52 percent of the total variability of α_b). The stochastic high-frequency variations (HFV) of α_b are characterized by a variance contribution $\hat{C}(0) = 0.099$ and a correlation length $\hat{J} = 2.96$ m. Note that about 60 percent of the HFV occurs at a scale smaller than the smallest lag distance of the sample set ($D_{\min} = 0.30$ m), and therefore appears as “white noise” or a “nugget effect.” In the case of α_K , the LFV of α_K are characterized by $\hat{C}_D = 0.3185$ (69 percent of the total variability of α_K); stochastic HFV of α_K are characterized by $\hat{C}(0) = 0.145$ and a correlation length $\hat{J} = 0.34$ m. There was no indication of variability at a scale less than D_{\min} (i.e., no nugget variance).

Linear regression analysis between the two sets of the uncorrelated residuals of α_K ($N[0.144, 0.979]$) and α_b ($N[0.150, 0.940]$) (slope = 0.62, intercept = 0.051, and $R^2 = 0.37$) implies that only 37 percent of the variability in α_K may be explained by the variability in α_b . These results suggest that the relatively good agreement between the two sets of the measured scaling factors is probably a joint consequence of the significant drift in the Hamra field and of spatial correlation between nearby measurements. The relatively poor agreement between the two sets of uncorrelated residuals of α reflects some basic differences between the spatial behavior of the $b(\theta)$ and the $K(\theta)$ functions, as indicated by the difference in structural models fitted to the sets of α_b and α_K .

Panoche Field

We analyzed the 120 laboratory-determined soil water retentivity $b(\theta)$ functions and the 120 field-determined soil hydraulic conductivity $K(\theta)$ functions from the study of Nielsen, Biggar, and Erh (1973) on the Panoche field, and the results are listed in table 8 as a summary of some statistical properties of the values of K and b and their logarithmic transforms for 11 discrete values of $s = \theta/\theta_s$. These values of $\ln K(s)$ and $\ln b(s)$ were used to calculate the two sets of α_K and α_b , respectively, using procedures described above.

The data in table 9 are the results of a conventional statistical analysis of α_b , $\ln \alpha_b$, α_K , and $\ln \alpha_K$. Based on the chi-square test and on the KS normality test, we conclude that both α_b and $\ln \alpha_b$ are normally distributed variates. As for α_K , both tests reject the null hypothesis but accept $\ln \alpha_b$ as normally distributed. Generally, for the range $0.75 \leq s \leq 1$, α_b varies between 0 and 2.5, and α_K varies between 0 and 5.5. Linear regression analysis between the two sets (slope = 1.456, intercept = -0.456, and $R^2 = 0.41$) implies that only 41 percent of the variability in α_K may be explained by the variability of α_b . These results differ from those of Warrick, Mullen, and Nielsen (1977), who found a higher degree of correlation in the analysis of the same data set using a different fitting procedure.

Using conventional statistical analysis, we analyzed the spatial variability of $\ln \alpha_b$ and $\ln \alpha_K$ instead of α_b and α_K . In the model-fitting process for $\ln \alpha_b$, the $E + C$, $S + C$, $E + L$, and $S + L$ models yielded AIC values of 66.9, 67.2, 70.48, and 70.35, respectively. For $\ln \alpha_K$, the same models yielded AIC values of 131.6, 132.8, 124.7, and 126.1. Thus we selected the $E + C$ model and the $E + L$ model for $\ln \alpha_b$ and $\ln \alpha_K$, respectively.

In table 10, we summarize the results of structural analysis, the cross-validation test, and analysis of the uncorrelated residuals for these two models. Again, as in the case of the Hamra field, the spatial correlation structures of $\ln\alpha_K$ and $\ln\alpha_b$ are quite distinct. The cross-validation test and the analysis of uncorrelated residuals suggest that, in both cases, the selected models are consistent with the data on $\ln\alpha_b$ and $\ln\alpha_K$, and that the assumption of normality for $\ln\alpha_b$ and $\ln\alpha_K$ is accepted (table 10c). In the case of $\ln\alpha_b$, the variability stems entirely from the stochastic HFV, characterized by $\hat{C}(0) = 0.251$ and a correlation length $\hat{J} = 4.82$ m. About 80 percent of this variability, however, occurs on a scale smaller than the smallest lag distance of the sample set ($D_{\min} = 0.3$ m) and appears as a nugget effect. In the case of $\ln\alpha_K$, for which a linear drift was identified (with $R^2 = 0.435$), the deterministic LFV are characterized by $\hat{C}_D = 0.658$ (30 percent of the total variability in $\ln\alpha_K$). The stochastic HFV are characterized by $\hat{C}(0) = 1.574$ and a correlation length of $\hat{J} = 0.305$ m. Only 3 percent of the HFV appears as a nugget effect at a scale less than $D_{\min} = 0.3$ m.

Linear regression analysis between the uncorrelated residuals of $\ln\alpha_K$ ($N[0.0328, 0.9989]$) and $\ln\alpha_b$ ($N[-0.0308, 0.9922]$) (slope = 0.662, intercept = 0.0367, and $R^2 = 0.44$) shows that only 44 percent of the variability of $\ln\alpha_K$ may be explained by the variability of $\ln\alpha_b$. Again, this relatively poor correlation between the two sets of $\ln\alpha$ values reflects some basic differences between the spatial structure of $b(s)$ and $K(s)$ as indicated by the different models that fitted the sets of $\ln\alpha_b$ and $\ln\alpha_K$ data (table 10).

TABLE 8. STATISTICAL CHARACTERISTICS (MEAN, COEFFICIENT OF VARIATION CV, AND VARIANCE σ^2 OF THE LOG-TRANSFORMED PARAMETER) OF THE HYDRAULIC PROPERTIES OF PANOCHE FIELD FOR DIFFERENT DEGREES OF WATER SATURATION s^*

Water saturation s	K			b		
	Mean	CV [†]	$\hat{\sigma}^2_{\ln K}$ [‡]	Mean	CV [†]	$\hat{\sigma}^2_{\ln b}$ [‡]
	<i>cm/br</i>			<i>cm H₂O</i>		
1.0	0.858	1.20	1.932	0	— [§]	— [§]
0.975	0.432	1.47	3.387	17.8	0.51	0.223
0.950	0.277	1.64	4.003	33.2	0.45	0.153
0.925	0.187	1.85	4.594	48.2	0.48	0.143
0.900	0.122	1.99	5.241	64.4	0.52	0.162
0.875	0.0815	2.23	6.250	82.6	0.55	0.194
0.850	0.0572	2.46	7.501	101.5	0.56	0.223
0.825	0.0414	2.69	9.183	120.2	0.56	0.236
0.800	0.0307	2.91	11.190	140.5	0.56	0.250
0.775	0.0226	3.13	13.390	160.2	0.55	0.251
0.750	0.0163	3.46	15.880	180.5	0.53	0.250

*Based on sample of $n = 120$.

[†]CV = Coefficient of variation.

[‡]For all water saturations but 1.0, null (normal) hypothesis is not rejected at the 0.05 level of significance (χ^2 test).

[§]No values were calculated.

TABLE 9. CONVENTIONAL STATISTICAL ANALYSIS OF THE SCALING FACTOR SETS (PANOCHE FIELD) CONSIDERING ALL SIX DEPTHS JOINTLY ($n = 120$)

Parameter	$\hat{\mu}$	$\hat{\sigma}^2$	\hat{k}_{sk}	\hat{k}_c	$\chi^2(df)$	D
α_b	1.000	0.223	1.350	7.297	4.6 (3)	.0777
$\ln\alpha_b$	-0.1089	0.229	-0.309	3.051	5.2 (3)	.0759
α_K	1.000	1.150	1.916	7.113	93.2 (3) [†]	.1799 [‡]
$\ln\alpha_K$	-0.607	1.622	-0.994	5.455	3.7 (3)	.0714

*Symbols are defined in table 6.

[†]Null (normal) hypothesis is rejected at the 0.05 level of significance.

[‡]Null (normal) hypothesis is rejected at the 0.10 level of significance.

TABLE 10. ANALYSIS OF THE SPATIAL VARIABILITY OF α_b AND α_K USING $n = 60$ VALUES OF BOTH α -SETS RANDOMLY SELECTED FROM THE SIX DIFFERENT SOIL DEPTHS (PANOCHE FIELD)*

<i>a. Structural analysis</i>								
Parameter	Model	\hat{C}_n	\hat{C}_o	\hat{a}				
$\ln\alpha_b$	$E + C$	0.2052 (.014)	0.0464 (.076)	3.41 (3.51)				
$\ln\alpha_K$	$S + L$	0.0535 (1.42)	1.521 (1.45)	0.681 (.72)				
<i>b. Cross validation</i>								
Parameter	Model	ME	MSE	MRE				
$\ln\alpha_b$	$E + C$	-0.0904	0.6337	1.272				
$\ln\alpha_K$	$S + L$	-0.0771	1.5840	1.146				
<i>c. Analysis of uncorrelated residuals</i>								
Parameter	Model	$\hat{\mu}$	$\hat{\sigma}^2$	\hat{k}_{sk}	\hat{k}_c	$\chi^2(df)$	D	SSR
$\ln\alpha_b$	$E + L$	-0.0308	0.9922	-0.515	2.423	4.56 (3)	0.0987	57.6
$\ln\alpha_K$	$S + L$	0.0328	0.9989	-0.923	5.144	4.21 (3)	0.1076	56.0

*Values in parentheses are the standard error of estimation (SE). Symbols are defined in tables 6 and 7.

ESTIMATION OF SCALING FACTORS WITH RELATIVE HYDRAULIC PROPERTIES

In principle, macroscopic Miller similitude should be applicable over the entire range of water content. In field soils, however, the saturated hydraulic conductivity may be controlled by water flow through large structural voids, or macropores, which drain at very small negative values of water pressure head, and therefore have little or no influence on water flow under unsaturated conditions. The models that we proposed for calculation of the soil hydraulic conductivity from data on the water retention

function commonly fail to predict the saturated hydraulic conductivity, and this indicates indirectly that the saturated hydraulic conductivity value is controlled to a great extent by flow in macropores. This conclusion applies to models based on the Kozeny approach (Averjanov 1950; Brooks and Corey 1964) as well as those based on capillary bundle theory (Burdine 1953; Childs and Collis-George 1950; Mualem 1976).

In our study, we analyze the correlation between the saturated hydraulic conductivity and the relative hydraulic conductivity $K_r(s) = K(s)/K_s$ of the Panoche field. The results of linear regression analysis (for 120 pairs of points) show that correlation between K_s and $K_r(s)$ decreases as s decreases. However, even at relatively high water saturation ($s = 0.975$), the correlation between K_s and $K_r(s)$ is barely significant ($R^2 = 0.038$). These results support the hypothesis that saturated hydraulic conductivity in field soils is controlled by structural voids, rather than by the entire continuum of pore sizes that controls the unsaturated hydraulic conductivity. Given these findings, scaling factors should be estimated from relative hydraulic properties instead of from the hydraulic properties themselves.

Hamra Field

For the Hamra field, using equation 12 with $m = 0$, we may define the relative properties as

$$b_r(\theta) = \frac{b\theta}{b_w} = \theta^{-1/\beta} \quad [14a]$$

and

$$K_r(\theta) = \frac{K(\theta)}{K_s} = \theta^{2+(2/\beta)} = \theta^\epsilon. \quad [14b]$$

Values of $K_r(\theta)$ and $b_r(\theta)$ calculated for 10 different values of $s = \theta/\theta_s$ ($s_i = 0.975 - 0.025 [i - 1]$ for $i = 1$ to $i = 10$, table 11) were used to determine the two sets of scaling factors by procedures already described.

The data presented in table 12 summarize the results of conventional statistical analysis of a_{b_r} and a_{K_r} and their logarithmic transformations. Both the chi-square test and the KS test reject the null (normal) hypothesis for a_{b_r} , a_{K_r} and their log transforms. The sample variances of the scaling factors derived from the relative hydraulic properties are smaller than those derived from the hydraulic properties and are very similar to each other (table 5). Linear regression analysis ($R^2 = 0.9976$, with intercept -0.0246 and slope 1.025) indicates that the two sets are highly correlated but not identical.

As mentioned above, proper application of linear regression analysis requires that each of the α sets comprises independent variates. The statistical estimation and validation procedures outlined above were used to analyze the correlation structures of these scaling sets. In table 13 we summarize the results of these analyses for the $E + L$ model, which produced the minimum value of AIC in the two cases. In contrast to the analyses of the original hydraulic properties, the spatial statistical characteristics of both sets of α derived from relative properties are very similar. Results of the cross-validation test indicate that the models selected are consistent with the data on the scaling factors. Analysis of the uncorrelated residuals demonstrates that, in both

cases, these residuals are distributed normally with zero mean and unit variance. This is in contrast to the results of the conventional statistical analysis of the original sets of α , which were skew-distributed (table 12). For both sets of α , linear drift was highly significant and contributed substantially to the total variation (LFV > HFV). The stochastic HFV of both α_{br} and α_{Kr} are characterized by a similar correlation length ($\hat{j} = 0.476$ m and $\hat{j} = 0.460$ m, respectively) and show no nugget effect (table 13). The estimated variances of each distribution are very similar, and linear regression analysis between the sets of uncorrelated residuals of α_{Kr} and α_{br} ($R^2 = 0.996$ with a slope of 1.006 and an intercept of 0.00003) implies that the two sets are highly correlated and almost identical.

The fact that both sets of α can be represented by the same structural model with essentially the same correlation length and with only slightly different variances $C(0)$

TABLE 11. STATISTICAL CHARACTERISTICS (MEAN, COEFFICIENT OF VARIATION CV, AND VARIANCE σ^2 OF THE LOG-TRANSFORMED PARAMETER) OF THE RELATIVE HYDRAULIC PROPERTIES OF HAMRA FIELD FOR DIFFERENT DEGREES OF WATER SATURATION s^*

Water saturation s	K_r			b_r		
	Mean	CV	$\hat{\sigma}^2_{\ln K}$	Mean	CV	$\hat{\sigma}^2_{\ln b_r}$
	<i>cm/br</i>			<i>cm H₂O</i>		
0.975	0.7716	0.196	0.0567	1.124	0.129	0.0135
0.950	0.6138	0.336	0.2360	1.293	0.298	0.0562
0.925	0.4981	0.445	0.5533	1.529	0.519	0.1317
0.900	0.4095	0.533	1.027	1.878	0.808	0.2442
0.875	0.3394	0.610	1.677	2.420	1.18	0.3985
0.850	0.2828	0.679	2.530	3.308	1.63	0.6004
0.825	0.2363	0.743	3.615	4.849	2.16	0.8567
0.800	0.1978	0.804	4.966	7.685	2.75	1.176
0.775	0.1655	0.862	6.629	13.230	3.34	1.567
0.750	0.1384	0.920	8.655	24.750	3.91	2.042

*Based on sample of size $n = 120$.

TABLE 12. CONVENTIONAL STATISTICAL ANALYSIS OF THE SCALING FACTOR SETS DERIVED FROM RELATIVE HYDRAULIC PROPERTIES (HAMRA FIELD)*

Parameter	$\hat{\mu}$	$\hat{\sigma}^2$	\hat{k}_{sk}	\hat{k}_c	$\chi^2(df)$	D
α_{br}	1.000	0.1890	-0.671	2.235	19.40 [†]	0.1345 [‡]
$\ln \alpha_{br}$	-0.1794	0.5339	-1.823	5.901	100.80 [†]	0.2141 [‡]
α_{Kr}	1.000	0.1989	-0.620	2.172	16.01 [†]	0.1308 [‡]
$\ln \alpha_{Kr}$	-0.1889	0.5634	-1.780	5.711	107.40 [†]	0.2040 [‡]

*Based on sample of size $n = 120$. Symbols are defined in table 6.

[†]Null (normal) hypothesis is rejected at the 0.05 level of significance.

[‡]Null (normal) hypothesis is rejected at the 0.10 level of significance.

suggests that α_{b_r} and α_{K_r} are proportional variables whose spatial variations are related to a unique spatial characteristic, represented by a unique or intrinsic variogram $\gamma_o(b)$

$$\gamma_{u_i}(b; s) = \gamma_o(b) \sigma_{u_i}^2(s), \text{ for } i = 1 \text{ to } i = 2 \tag{15}$$

(Russo 1986), where $u_i = u_i(s)$ denotes either α_{K_r} or α_{b_r} , and $\sigma_{u_i}^2(s)$ is the variance of u_i . Equations 3 and 11a, when used with relative hydraulic properties, lead to the values of α_{K_r} and α_{b_r} given by the equations

$$\alpha_{K_r}(s) = [K_r(s)/K_r^*(s)]^{1/2} \tag{16a}$$

and

$$\alpha_{b_r}(s) = b_r^*(s)/b_r(s), \tag{16b}$$

where $K_r^*(s)$ and $b_r^*(s)$ are defined by equations 13a and 13b, respectively, but using relative properties. The variances of α_{K_r} and α_{b_r} may be estimated from equation 16 by the expressions

$$\sigma_{\alpha_{K_r}}^2(s) = \sigma_{K^{1/2}}^2(s) [K_r^*(s)]^{-1} \tag{17a}$$

and

$$\sigma_{\alpha_{b_r}}^2(s) = \sigma_{b^{-1}}^2(s) [b_r^*(s)]^2 \tag{17b}$$

(Clifford 1973), where $\sigma_{K^{1/2}}^2$ is the variance of $K_r(s)^{1/2}$ and $\sigma_{b^{-1}}^2$ is the variance of $b_r(s)^{-1}$ (equation 16). For the relevant range of water saturation (s_{\min} , s_{\max}), an estimate of the total variance of α may be obtained from the equation

$$\sigma_{\alpha}^2(s_{\min}, s_{\max}) = \sum_{i=1}^{n_s} \sigma_{\alpha}^2(s) \cdot \Delta w, \tag{18}$$

TABLE 13. ANALYSIS OF THE SPATIAL VARIABILITY OF α_{b_r} AND α_{K_r} USING $n = 60$ VALUES OF BOTH α -SETS RANDOMLY SELECTED FROM THE FOUR DIFFERENT SOIL DEPTHS (HAMRA FIELD)*

<i>a. Structural analysis</i>								
Parameter	Model	\hat{C}_n	\hat{C}_o	\hat{a}				
α_{b_r}	E + L	0 (—)	0.0712 (.144)	0.3365 (.150)				
α_{K_r}	S + L	0 (—)	0.0722 (.146)	0.3255 (.148)				
<i>b. Cross validation</i>								
Parameter	Model	ME	MSE	MRE				
α_{b_r}	E + L	-0.01234	0.2548	1.124				
α_{K_r}	S + L	-0.00867	0.2565	1.118				
<i>c. Analysis of uncorrelated residuals</i>								
Parameter	Model	$\hat{\mu}$	$\hat{\sigma}^2$	\hat{k}_{sk}	\hat{k}_c	$\chi^2(df)$	D	SSR
α_{b_r}	E + L	0.1213	0.9853	-0.353	3.06	1.0 (3)	0.0620	56.0
α_{K_r}	S + L	0.1258	0.9842	-0.297	3.12	2.1 (3)	0.0591	56.0

*Symbols are defined in tables 6 and 7. Values in parentheses are the standard error of estimation (SE). If the value is zero, there is no standard error.

where $\sigma_\alpha^2(s)$ is the variance of α at a given s (equation 17a or equation 17b) and Δw is an error-free weighting factor defined as $\Delta w = 1/n_s$, where n_s is the number of s values used in the calculation of $K(s)$ or $b(s)$ and $\sigma_\alpha^2(s)$.

In the case of the Hamra field, where equations 12a and 12b were used to describe $b(\theta)$ and the $K(\theta)$, $K_r(s)^{1/2}$ and $b_r(s)^{-1}$ are given by the equations

$$[K_r(s)]^{1/2} = [\theta(s)]^{\epsilon/2} \tag{19a}$$

and

$$[b_r(s)]^{-1} = [\theta(s)]^{1/\beta} \tag{19b}$$

The variances of these functions may be evaluated approximately with the procedure for expanding the total differential of a two-valued function (Clifford 1973) to first order as

$$\begin{aligned} \sigma_{K^{1/2}(s)}^2 &= \left[\frac{\epsilon}{2} \theta(s)^{(\epsilon/2)-1} \right]^2 \sigma_{\theta(s)}^2 + [\theta(s)^{\epsilon/2} \ln \theta(s)]^2 \sigma_{\epsilon/2}^2 \\ &+ 2 \left[\frac{\epsilon}{2} \theta(s)^{\epsilon-1} \ln \theta(s) \right] \cdot \text{cov}[\epsilon/2, \theta(s)] \end{aligned} \tag{20a}$$

and

$$\begin{aligned} \sigma_{b^{-1}(s)}^2 &= \left[\frac{1}{\beta} \theta(s)^{(1/\beta)-1} \right]^2 \sigma_{\theta(s)}^2 + [\theta(s)^{1/\beta} \ln \theta(s)]^2 \sigma_{1/\beta}^2 \\ &+ 2 \left[\frac{1}{\beta} \theta(s)^{(2/\beta)-1} \ln \theta(s) \right] \cdot \text{cov}[1/\beta, \theta(s)]. \end{aligned} \tag{20b}$$

Examination of equations 17 to 20 reveals three basic points relative to scaling hydraulic properties: .

1. Soils whose properties can be represented by equation 14 at different spatial locations may be regarded as "strictly similar media," if and only if $\epsilon/2 = 1/\beta$. According to equation 12, this equality is satisfied only when $m = -2$, which means that the relative hydraulic conductivity $K_r(b_r)$ is a deterministic function everywhere equal to $K_r(b_r) = b^{-2}$. In general, however, when $m \neq -2$, $K_r(b_r)$ is a stochastic function characterized by the relationship

$$K_r(b_r) = b_r^{-\eta}, \tag{21}$$

where $\eta = 2(\beta + m) + 2$ is a stochastic variable (Russo and Bresler 1981).

2. The strict applicability of the macroscopic Miller similitude (validated by examination of the agreement between the sets of α_K and α_b) is improved as the value of β decreases (e.g., in a medium with a relatively wide and continuous pore size distribution). Even for very small values of $\beta > 0$, however, the two sets of α are not identical so long as $m \neq 2$.

3. Both α_{b_r} and α_{K_r} are functions of the degree of water saturation s , since the variances of both $K^{1/2}(s)$ and $b_{r-1}(s)$ depend on s . The higher the range of saturation, the larger are the variances of α_{b_r} or α_{K_r} . This means that the application of scaling factors to transport processes (e.g., Bresler and Dagan 1979; Dagan and Bresler 1979) should be limited to the same range of water saturation as was used to estimate scaling factors.

The above analysis suggests that a second stochastic parameter in addition to α is required to scale both $b_r(s)$ and $K_r(s)$. For media in which the functional relationship in equation 21 applies at any given location, the stochastic parameter η may be used as a second scaling factor.

To determine whether media scaled by equations 16b and 21 account for all of the observed variability in K_r and b_r , one may define a new α_{K_r} by the equation

$$\alpha_{K_r} = \alpha_{b_r} = [K_r(s)/K_r^*(s)]^{1/\eta}, \quad [22]$$

where $K_r^*(s)$ is defined by the requirement that $E[\alpha_{K_r}] = 1$ as

$$K_r^*(s) = \left\{ \int_0^\infty [K_r(s)]^{1/\eta} f[K_r(s)] dK_r \right\}^\eta \quad [23a]$$

or

$$K_r^*(s) = [b_r^*(s)]^{-\eta}. \quad [23b]$$

Note that K_r^* is no longer a “reference site,” but is now dependent on η . Alternatively, K_r could be used as the second scaling factor using equation 23b to generate it from η . With either approach, we are left with two scaling factors for b_r and K_r . The validity of each approach is ascertained by the degree to which α_{K_r} , defined by equation 22 is similar to α_{b_r} defined by equation 16b.

The analysis of spatial structure for $K_r(s)$ was repeated using equation 22 to define α_{K_r} in terms of η . For the Hamra field, the results of conventional statistical analysis of η ($\hat{\mu} = 3.355$, $\hat{\sigma}^2 = 1.412$, $\hat{k}_s = 1.83$, $\hat{k}_c = 7.69$ and $\chi^2[3] = 60$) suggest that η is highly skewed and cannot be described by either a normal or a lognormal ($\chi^2[3] = 14$) distribution. Results of structural analysis (validated by the cross-validation test and analysis of the uncorrelated residuals) imply that the spatial variability of η is described best by the $E + L$ model (AIC = 158.7). The stochastic HFV of η are characterized by $\hat{C}(0) = 0.7125$ (with no nugget effect) and by an integral scale of $\hat{J} = 0.47$ m. The deterministic linear drift was highly significant ($R^2 = 0.941$) and the LFV of η are characterized by $\hat{C}_D = 0.8394$ (54 percent of the total variability of in η , with $\hat{\sigma}^2 = 1.552$). Note that the spatial structures of η and α_{b_r} (or α_{K_r}) are very similar, in the sense that about 50 percent of the total variability of each one stems from the presence of a deterministic drift, whereas the rest of the variability is characterized by essentially the same correlation scale. Measured η values were used to calculate a new set of α_{K_r} using equation 22. The set of values thus obtained was statistically identical to the α_{b_r} set (table 12).

Panoche Field

In the Panoche field experiment, water retention curves were determined in the laboratory over a very limited range of water pressure heads (0 to -200 cm water), which for this soil essentially resulted in a linear $\theta(b)$ relationship. Therefore, to define a relative $b_r(s)$ function, $b(0.98)$ was selected arbitrarily as an air-entry value b_ω so that $b_r(s) = b(s)/b(0.98)$. The field-measured hydraulic conductivity values K_s from the steady state infiltration phase of the experiment and the $K(\theta)$ values from the redistribution phase were used to define a relative hydraulic conductivity, $K_r(s) = K(s)/K_s$. The data in table 14 summarize the mean and variance of K_r and b_r for 10 different degrees of water saturation. As was the case for the Hamra field, the variability in $K_r(s)$ is smaller than the variability in $K(s)$, since the contribution of K_s to the variance has been removed.

Values of the relative hydraulic properties for the 10 values of water saturation shown in table 14 were used to calculate a set of scaling factors α_{b_r} and α_{K_r} , as defined by equation 16. In table 15, we summarize the results of a conventional statistical analysis of the α -sets and their logarithmic transformations. It is clear that the resultant α -sets using relative properties are less variable than the α_b and α_K values determined previously with $b(\theta)$ and $K(\theta)$ (table 9). Moreover, relative property α -sets are distributed normally, as in the Hamra field. Linear regression analysis (slope 1.045, intercept -0.04487 , and $R^2 = 0.41$) suggests that the use of relative hydraulic

TABLE 14. STATISTICAL CHARACTERISTICS (MEAN, COEFFICIENT OF VARIATION CV, AND VARIANCE σ^2 OF THE LOG-TRANSFORMED PARAMETER) OF THE RELATIVE HYDRAULIC PROPERTIES OF PANOCHE FIELD FOR DIFFERENT DEGREES OF WATER SATURATION s ($n = 120$)

Water saturation s	K_r			b_r		
	Mean	CV	$\hat{\sigma}^2_{\ln K}$	Mean	CV	$\hat{\sigma}^2_{\ln b_r}$
	<i>cm/br</i>			<i>cm H₂O</i>		
0.975	0.4514*	0.535	0.918	1.227	0.055	0.0030
0.950	0.2821*	0.736	1.673	2.436	0.268	0.0624*
0.925	0.1851	0.945	2.310	3.655	0.391	0.1289*
0.900	0.1204	1.068	2.989	5.012	0.497	0.1976*
0.875	0.0798	1.268	3.951	6.577	0.593	0.2712
0.850	0.0561	1.482	5.215	8.181	0.627	0.3255
0.825	0.0403	1.729	6.842	9.816	0.652	0.3640*
0.800	0.0295	2.020	8.699	11.600	0.670	0.3981*
0.775	0.0214	2.271	10.86	13.370	0.671	0.4192*
0.750	0.0153	2.458	13.32	15.110	0.672	0.4262*

*Null (normal) hypothesis is not rejected at the 0.05 level of significance (χ^2 test).

TABLE 15. CONVENTIONAL STATISTICAL ANALYSIS OF THE SCALING FACTOR SETS DERIVED FROM RELATIVE HYDRAULIC PROPERTIES (PANOCHE FIELD)*

Parameter	$\hat{\mu}$	$\hat{\sigma}^2$	\hat{k}_{sk}	\hat{k}_c	$\chi^2(df=3)$	D
a) α_{b_r}	1.000	0.1981	0.695	3.19	3.1	0.0623
$\ln \alpha_{b_r}$	-0.103	0.2167	-0.253	2.34	8.3 [†]	0.0833
b)‡ α_{K_r}	1.000	0.464	0.856	3.38	7.6	0.0843
$\ln \alpha_{K_r}$	-0.3282	1.022	-2.15	11.71	14.6 [†]	0.1173 [§]
c)¶ α_{K_r}	1.000	0.2278	0.631	3.03	3.8	0.0716
$\ln \alpha_{K_r}$	-0.0131	0.2985	-0.581	3.11	2.9	0.0761

*Based on sample of size $n = 120$. Symbols are defined in table 6.

[†]Null hypothesis is rejected at the 0.05 level of significance.

[‡]Calculated using equation 16a.

[§]Null hypothesis is rejected at the 0.10 level of significance.

[¶]Calculated using equation 22.

properties to estimate the α -sets only slightly improved the agreement between the two α -sets, as compared with the agreement between the α_K and the α_b sets (slope 1.456, intercept -0.456 , and $R^2 = 0.41$).

To test the applicability of equations 21 and 22 to the Panoche field, values of $\eta = -d \log K_r / d \log b_r$ were estimated by linear regression analysis of the log-transforms of K_r and b_r . For most of 120 locations in the Panoche field, the model $K_r(b_r)$ function in equation 21 adequately describes the actual $K_r(b_r)$ data, as indicated by the relatively high values of the coefficient of determination ($R^2 > 0.85$). The resultant distribution of η values ($\hat{\mu} = 2.544$, $\hat{\sigma}^2 = 1.439$, $\hat{k}_s = 3.086$, $\hat{k}_c = 19.6$) was highly skewed and the null (normal) hypothesis was rejected ($\chi^2[3] = 34.2$). Conversely, $\ln \eta$ was found to be normally distributed ($\chi^2[3] = 4.7$) with $\hat{\mu} = 0.8516$, $\hat{\sigma}^2 = 0.1539$, $\hat{k}_{sk} = 0.325$, and $\hat{k}_c = 4.76$.

The structural analysis suggests that the spatial variability of $\ln \eta$ is described best by the $E + L$ model (AIC = 160.1) with zero correlation scale ("pure nugget effect"). The stochastic HFV of $\ln \eta$ are characterized by $\hat{C}(0) = \hat{C}_n = 0.1294$, which stems entirely from property variations at a scale less than 0.3 m. A significant linear drift ($R^2 = 0.88$) was detected, whose contribution to the total variance is characterized by $\hat{C}_D = 0.0282$ (18 percent of the total variability of $\ln \eta$).

Values of η were used to estimate another set of α_{K_r} using equation 22. Results of the statistical analysis of the resultant α_{K_r} are given in table 15c, which indicates that the new α_{K_r} set is normally distributed and less variable than that derived by the traditional approach assuming a deterministic $\eta = 2$ for all sites (table 15b). Linear regression analysis (slope 0.833, intercept 0.152, and $R^2 = 0.60$) suggests that the use of equation 21 improved considerably the agreement between α_{b_r} and the α_{K_r} sets.

We then conducted a detailed structural analysis of the scaling factors derived from the relative hydraulic properties. Based on table 15, the spatial structures of the α -sets were analyzed instead of their logarithmic transforms. Results of structural analysis and the associated validation tests of the three α -sets in table 15 are summarized in table 16. A comparison of the results in table 16 with those in table 10 suggests that the spatial structures of the α -sets derived from the relative hydraulic properties are different from those derived from the hydraulic properties themselves. A significant linear drift was detected for α_{b_r} and α_{K_r} , both when the original scaling equations were used (equation 16) and when the scaling factor η was introduced to define α_{K_r} (equation 22). In contrast to the Hamra field, significant differences in the spatial structures of α_{b_r} and α_{K_r} still exist even when η is allowed to vary at each measurement site. One possible explanation for these differences is that, in the Panoche study, $K(\theta)$ was measured in the field and $b(\theta)$ in the laboratory, whereas all measurements in the Hamra study were made with a permeameter.

In spite of the failure to achieve perfect agreement between α_{b_r} and α_{K_r} with equation 22, the improvement over traditional scaling (equation 16) was significant. Analysis of the uncorrelated residuals of α_{K_r} and α_{b_r} that were determined from equation 16 gives $R^2 = 0.29$ with a slope of 0.887 and an intercept of 0.014, whereas the set defined with equation 22 gave $R^2 = 0.61$ with a slope of 0.946 and an intercept of -0.002 . Since the values of η were independently determined from the data, this improved agreement offers convincing evidence that the more general scaling model is applicable to the Panoche field as well.

TABLE 16. STRUCTURAL ANALYSIS OF SCALING FACTORS DERIVED FROM RELATIVE HYDRAULIC PROPERTIES (PANOCHÉ FIELD)*

<i>a. Structural analysis</i>						
Parameter	Model	\hat{C}_n	\hat{C}_o	\hat{a}	AIC	
α_{b_r}	S + L	0.1063 (.035)	0.0232 (.021)	15.121 (9.8)	55.6	
$\alpha_{K_r}^\dagger$	E + L	0.3199 (.125)	0.0255 (.117)	4.637 (22.3)	116.0	
$\alpha_{K_r}^\ddagger$	S + L	0.0878 (.039)	0.1127 (.057)	3.315 (3.34)	74.0	

<i>b. Cross validation</i>				
Parameter	Model	ME	MSE	MRE
α_{b_r}	S + L	0.0756	0.4464	1.266
$\alpha_{K_r}^\dagger$	E + L	-0.0580	0.7645	1.245
$\alpha_{K_r}^\ddagger$	S + L	0.0383	0.4087	1.181

<i>c. Analysis of uncorrelated residuals</i>								
Parameter	Model	$\hat{\mu}$	$\hat{\sigma}^2$	\hat{k}_{sk}	\hat{k}_c	$\chi^2(df)$	D	SSR
α_{b_r}	S + L	0.1747	0.9395	0.540	3.43	1.21 (3)	0.078	55.95
$\alpha_{K_r}^\dagger$	E + L	0.1088	0.9843	0.219	2.56	1.86 (3)	0.084	55.80
$\alpha_{K_r}^\ddagger$	S + L	0.1729	0.9453	0.396	2.67	2.29 (3)	0.059	56.00

*Values in parentheses are the standard error of estimation (SE). Symbols are defined in tables 6 and 7.

†Calculated using equation 16a.

‡Calculated using equation 22.

SUMMARY AND CONCLUSIONS

We analyzed the possibility of introducing a single stochastic scaling parameter α to describe the spatial variability of soil hydraulic properties, using the soil hydraulic properties of the Hamra field (Russo and Bresler 1981) and the Panoche field (Nielsen, Biggar, and Erh 1973). In the traditional approach (Peck, Luxmoore, and Stolzy 1977; Russo and Bresler 1980; Warrick, Mullen, and Nielsen 1977), sets of scaling factors are estimated from the $b(s)$ and $K(s)$ functions. For "perfectly similar media," the two sets of α should be identical. Even though the sets of α in these studies were found to be correlated (table 2), they possessed different statistical properties, and were not identical. Results of structural analyses of the sets of α from the two fields suggested that the spatial structures of the two α -sets are quite distinct, reflecting the different spatial behavior of the $b(\theta)$ and the $K(\theta)$ functions. Moreover, there was poor correlation between the uncorrelated residuals of the α -sets, indicating that part of the high correlation between the α -sets found in earlier work must stem from the presence of an undetected drift and from correlation between nearby measurements.

Under field conditions, the saturated hydraulic conductivity is controlled by the flow of water through large structural voids (macropores), which drain at very small negative values of water pressure. Because of this, we tried eliminating K_s by using

relative hydraulic properties instead of the hydraulic properties themselves to estimate the scaling factor sets. For the Hamra field, for which we assumed that the hydraulic properties could be described by the model of Brooks and Corey (1964), we found the resultant sets of scaling factors to be highly correlated ($R^2 = 0.996$) with the same spatial structure, but with slightly different variance. By examining the relationships between the two α -sets implied by the Brooks and Corey (1964) model we saw that (1) in general, both sets will be functions of the range of water saturation values used to estimate them, (2) the correlation between the two sets can be improved for media with broad pore-size distributions, and (3) the two sets will be identical if and only if the relative hydraulic conductivity function $K_r(b_r)$ is described by the deterministic function $K_r(b_r) = b_r^{-2}$ ("strictly similar media").

This analysis suggests that, for media that are not well described by $K_r = b_r^{-2}$, a scaling factor would be required in addition to α in order to achieve agreement between scaled values of $b_r(\theta)$ and $K_r(\theta)$ at all points. A general model $K_r = b_r^{-\eta}$ was proposed, with η as a second stochastic scaling factor for media that do not obey the restrictive assumptions of macroscopic Miller similitude. In the Hamra field, this modified scaling procedure produced perfect agreement between the scaling hydraulic properties. In the Panoche field, with values of η determined from linear regression analysis of the logarithmic transformations of K_r and b_r , agreement was improved considerably between the scaled hydraulic properties as compared to the more restrictive scaling procedure. In contrast to the Hamra field, however, there remained some significant differences between the scaled properties. These differences may have been artifacts of the different methods used to estimate the $b(s)$ and the $K(s)$ functions for the Panoche field.

The results of our analysis suggest that in any transient transport problem involving both $K(s)$ and $b(s)$, the description of their spatial variability requires the use of at least three stochastic variates— K_s , α , and η —not α alone.

ACKNOWLEDGMENT

The authors wish to thank the Electric Power Research Institute and the Southern California Edison Company for their partial financial support of this project.

LITERATURE CITED

- AITCHESON, J., and J. A. C. BROWN
1976. *The lognormal distribution*. Cambridge, England: Cambridge University Press.
- AVERJANOV, S. F.
1950. About permeability of subsurface soils in case of incomplete saturation. Eng. Collect. 7.
- BRESLER, E., and G. DAGAN
1979. Solute dispersion in unsaturated heterogeneous soil at field scale. 2. Applications. Soil Sci. Soc. Am. J. 43:467-72.
1981. Convective and pore scale dispersive solute transport in unsaturated heterogeneous fields. Water Resour. Res. 17:1683-93.
1983a. Unsaturated flow in spatially variable fields. 2. Application of water flow models to various fields. Water Resour. Res. 19:421-28.
1983b. Unsaturated flow in spatially variable fields. 3. Solute transport models and their application to two fields. Water Resour. Res. 19:429-35.
- BRESLER, E., D. RUSSO, and R. D. MILLER
1978. Rapid estimate of unsaturated hydraulic conductivity function. Soil Sci. Soc. Am. J. 42:170-72.
- BROOKS, R. H., and A. T. COREY
1964. Hydraulic properties of porous media. Colo. State Univ. Fort Collins Hydrol. Pap. 3.
- BURDINE, N. T.
1953. Relative permeability calculation from size distribution data. Trans. Am. Inst. Min. Eng. 198:71-78.
- CHILDS, E. C., and N. COLLIS-GEORGE
1950. The permeability of porous materials. Proc. R. Soc. London Ser. A 201:392-405.
- DAGAN, G., and E. BRESLER
1979. Solute dispersion in unsaturated heterogeneous soil at field scale. 1. Theory. Soil Sci. Soc. Am. J. 43:461-67.
1983. Unsaturated flow in spatially variable fields. 1. Derivation of models of infiltration and redistribution. Water Resour. Res. 19:413-20.
- ELRICK, D. E., J. H. SANDRETT, and E. E. MILLER
1959. Tests of capillary flow scaling. Soil Sci. Soc. Am. J. 23:329-32.
- HALD, A.
1952. *Statistical theory with engineering applications*. New York: Wiley.
- HUFF, D. D., R. J. LUXMOORE, J. B. MANKIN, and C. L. BEGOVICH
1976. *TEHM: A terrestrial ecosystem hydrology model*. Rep. ORNL/NSF/EATC-27, Oak Ridge, Tennessee: Oak Ridge Nat. Lab.
- JURY, W. A.
1985. Spatial variability of soil physical parameters in solute migration: A critical literature review. *EPRI Topical Rep. EA4228*. Palo Alto: Electric Power Research Institute.
- JURY, W. A., D. RUSSO, G. SPOSITO, and H. ELABD
1987. The spatial variability of water and solute transport properties in unsaturated soil. I. Analysis of property variation and spatial structure with statistical models. *Hilgardia* 55:(4) (this issue).
- KITANIDIS, P. K., and R. W. LANE
1985. Maximum likelihood parameter estimation of hydrologic spatial processes by the Gauss-Newton method. *J. Hydrol.* 79:53-71.
- KLUTE, A., and G. E. WILKINSON
1958. Some tests of the similar media concept of capillary flow. I. Reduced capillary conductivity and moisture characteristic data. *Soil Sci. Soc. Am. Proc.* 22:278-81.
- LUXMOORE, R. J., and M. L. SHARMA
1980. Runoff response to soil heterogeneity: Experimental and simulation comparisons for two contrasting watersheds. *Water Resour. Res.* 16:675-84.
- MILLER, E. E.
1980. Similitude and scaling of soil water phenomena. In *Applications of soil physics*, ed. D. Hillel, 300-318. New York: Academic Press.

- MILLER, E. E., and R. D. MILLER
1956. Physical theory for capillary flow phenomena. *J. Appl. Phys.* 27:324-32.
- MUALEM, Y.
1976. A new model for predicting the hydraulic conductivity of unsaturated porous media. *Water Resour. Res.* 12:513-22.
- NIELSEN, D. R., J. W. BIGGAR, and K. T. ERH
1973. Spatial variability of field measured soil water properties. *Hilgardia* 42(7): 215-59.
- PECK, A. J., R. J. LUXMOORE, and L. J. STOLZY
1977. Effects of spatial variability of soil hydraulic properties in water budget modeling. *Water Resour. Res.* 13:348-54.
- PHILIP, J. R.
1969. The theory of infiltration. *Adv. Hydrosoci.* 5:215-90.
- RAO, P. S. C., R. E. JESSUP, A. C. HORNSBY, D. K. CASSEL, and W. A. POLLANS
1983. Scaling soil microhydrologic properties of Lakeland and Konowa soils using similar media concepts. *Agric. Water Manage.* 6:277-90.
- REICHARDT, K., P. L. LIBARDI, and D. R. NIELSEN
1975. Unsaturated hydraulic conductivity determination by a scaling technique. *Soil Sci.* 120:165-68.
- REICHARDT, K., D. R. NIELSEN, and J. W. BIGGAR
1972. Scaling of horizontal infiltration into homogeneous soils. *Soil Sci. Soc. Am. J.* 36:241-45.
- RUSSO, D., and E. BRESLER
1980. Scaling soil hydraulic properties of a heterogeneous field. *Soil Sci. Soc. Am. J.* 44:681-83.
1981. Soil hydraulic properties as stochastic processes. I. An analysis of field spatial variability. *Soil Sci. Soc. Am. J.* 45:682-87.
1982. A univariate versus a multivariate parameter distribution in a stochastic-conceptual analysis of unsaturated flow. *Water Resour. Res.* 18:483-88.
- SHARMA, M. L., G. A. GANDER, and C. G. HUNT
1980. Spatial variability of infiltration in a watershed. *J. Hydrol.* 45:101-22.
- SIMMONS, C. S., D. R. NIELSEN, and J. W. BIGGAR
1979. Scaling of field-measured soil-water properties. *Hilgardia* 47(4):77-174.
- SPOSITO, G., and W. A. JURY
1985. Inspectional analysis in the theory of water flow through unsaturated soil. *Soil Sci. Soc. Am. J.* 49:791-98.
- TILLOTSON, P., and D. R. NIELSEN
1984. Scale factors in soil science. *Soil Sci. Soc. Am. J.* 48:953-59.
- WARRICK, A. W., and A. AMOOZEGAR-FARD
1980. Infiltration and drainage calculations using spatially scaled hydraulic properties. *Water Resour. Res.* 15:1116-20.
- WARRICK, A. W., G. J. MULLEN, and D. R. NIELSEN
1977. Scaling field measured soil hydraulic properties using a similar media concept. *Water Resour. Res.* 13:355-62.
- WARRICK, A. W., and D. R. NIELSEN
1980. Spatial variability of soil physical properties in the field. In *Applications of soil physics*, ed. D. Hillel, 319-344. New York: Academic Press.
- WILKINSON, G. E., and A. KLUTE
1959. Some tests of the similar media concept of capillary flow. II. Flow systems data. *Soil Sci. Soc. Am. J.* 23:434-37.
- YOUNGS, E. G., and R. I. PRICE
1981. Scaling of infiltration behavior in dissimilar porous media. *Water Resour. Res.* 17:1065-70.

The University of California, in compliance with the Civil Rights Act of 1964, Title IX of the Education Amendments of 1972, and the Rehabilitation Act of 1973, does not discriminate on the basis of race, creed, religion, color, national origin, sex, or mental or physical handicap in any of its programs or activities, or with respect to any of its employment policies, practices, or procedures. The University of California does not discriminate on the basis of age, ancestry, sexual orientation, marital status, citizenship, medical condition (as defined in section 12926 of the California Government Code), nor because individuals are disabled or Vietnam era veterans. Inquiries regarding this policy may be directed to the Personnel Studies and Affirmative Action Manager, Division of Agriculture and Natural Resources, 2120 University Avenue, University of California, Berkeley, California 94720, (415) 644-4270.

Continued from inside front cover.

component than the Panoche field of Nielsen, Biggar, and Erh (1973). The stochastic component of $\ln K_s$ in the Bet-Dagan field possessed a large nugget variance (40 percent of total) and was characterized by an integral scale of $J = 14.5$ m, as compared with $J = 8.1$ m and a small nugget variance (13 percent of total) in the Panoche field.

II. Scaling Models of Water Transport

In this paper, we examine the possibility of introducing a single stochastic scaling factor α , derived from macroscopic Miller similitude, to describe the spatial variability of soil hydraulic properties. Most of the information available allowed only a conventional statistical analysis of the scaling factors derived from different soil properties. The field studies of Nielsen, Biggar, and Erh (1973) and Russo and Bresler (1981) were suitable also for more detailed structural analyses. Results of these analyses suggested that the spatial structure of the α -set derived from the hydraulic conductivity function $K(\theta)$ is different from that of the α -set derived from the water retentivity function $b(\theta)$, reflecting the different spatial structures of the $K(\theta)$ and the $b(\theta)$ functions. Consequently, the statistical relationship between the uncorrelated residuals of the two α -sets was rather weak. For the Hamra field of Russo and Bresler (1981), the use of relative hydraulic properties to estimate the scaling factor sets considerably improved the correlation between the α -sets, which had essentially the same spatial structure but slightly different variances.

In this study, where the soil hydraulic properties are assumed to be described by the model of Brooks and Corey (1964), analytical expressions for the variances of the two different α -sets indicated that (1) both α -sets are dependent on the range of water saturation that is used to estimate them, (2) the correlation between the two sets will improve in media with a wide pore-size distribution, and (3) the two sets will be identical if and only if the relative hydraulic conductivity function $K_r(b_r)$ is described by a deterministic function, $K_r(b_r) = b_r^{-2}$. This result suggested that, in general, a second scaling factor for K_r is required for media that are not characterized by this single deterministic relationship.

A more general $K_r(b_r)$ relation, defined by $K_r = b_r^{-\eta}$, was introduced using η as a second stochastic variable. In this representation, the α scaling factor for K_r is defined by $K_r/K_r^* = \alpha^\eta$ instead of α^2 as in macroscopic Miller similitude. For the Hamra field, the resultant new α -set was identical to the α -set derived from the relative retentivity function. For the Panoche field, using the values of η to estimate the scaling factor from the relative hydraulic conductivity function considerably improved the correlation and the similarity between the two α -sets, but did not render them identical. The results of our analysis suggest that, for transient water flow, describing the spatial variability of $K(\theta)$ and $b(\theta)$ requires at least three stochastic variates: K_s , α , and η .

HILGARDIA Editorial Board

Edward S. Sylvester, Chairman, Berkeley
(entomology, insecticides, ecology, environmental toxicology)

Peter Berck, Associate Editor, Berkeley
(economics, statistics, resource management)

Harry W. Colvin, Associate Editor, Davis
(animal science, physiology, breeding, zoology, genetics)

Donald J. Durzan, Associate Editor, Davis
(tree fruit and nut crops)

Walter G. Jennings, Associate Editor, Davis
(food science, nutrition, and chemistry)

John Letey, Associate Editor, Riverside
(soils, plant nutrition, agronomy, agricultural engineering, water)

(field and row crops)

Irwin P. Ting, Associate Editor, Riverside
(botany, plant physiology, biochemistry)

Richard V. Venne, Managing Editor, Berkeley